AUTONOMOUS PROCESSING OF SIDESCAN SONAR IMAGERY FOR UNMANNED UNDERWATER VEHICLES

L.J. Hamilton and J. Cleary

Defence Science and Technology Group
Eveleigh, NSW 2015, Australia
Email: les.hamilton@dsto.defence.gov.au

Abstract

Unmanned Underwater Vehicles can autonomously obtain high quality sidescan sonar backscatter swathe imagery of the seabed by traversing pre-programmed tracks at a set height above the bottom where they are relatively undisturbed by wave action. Some survey activities could be more efficient if the UUVs had some machine intelligence or decision making capability. For example, UUVs could be programmed to survey seabeds of particular interest at slower speeds to obtain more detail, or might resurvey particular areas using more detailed search patterns. Onboard processing for this purpose requires fast algorithms and robust decisions. Ongoing work in autonomously characterizing sidescan sonar imagery for seabed type is described. Humans can readily recognize patterns and textures indicative of particular seabed types, for example, sand has characteristic ripple patterns. Can Unmanned Underwater Vehicles be given the capability to autonomously mimic human visual perception?

1. Introduction

Unmanned Underwater Vehicles (UUVs) could perform some tasks more efficiently if they were able to make on-board decisions based on inputs from their environmental sensors. Recognition that seabed clutter in incoming sidescan sonar swathe data was too high, or that seabeds were too undulatory (resulting in unensonified shadow areas) for successful searches of objects on the seabed could enable UUVs to choose not to run followup object detection software, or to change search strategy. For example they could rescan areas with runs across recognized sandwave lines, not along them, in order to maximise unobscured seabed coverage. This presentation seeks methods of processing and interpreting sidescan sonar data which could enable such autonomous decisions. Knowledge of the bathymetry in an area could make the sandwave example a relatively simple problem, but sidescan sonar explicitly provides depth information only along track, and not across the sonar swathe. However, statistics of the acoustic seabed backscatter response stimulated by the sidescan sonar can enable remote sensing inferences of seabed type, seabed clutter, and directionality of seabed features. UUVs tasked to find and map the extent of particular habitat types such as rock or seagrass could make direct use of this information to initiate and optimise autonomous actions.

2. Sidescan Sonar

For sidescan sonar the received acoustic signal is a backscatter intensity or amplitude time series received from a long thin strip of seabed perpendicular to a transducer array. These backscatter series are used in real-time to construct an image of the seabed similar to black and white video. Observers examine this imagery for seabed features and objects on the seabed. The backscatter responses for scan lines can be processed to infer seabed type, either through feature analysis or by treating the responses as discrete geometrical entities or curves (Hamilton and Parnum 2013). Statistical characterization of scan lines can identify some seabed types and changes in seabed type. However, autonomous detection of the position and scale of objects on the seabed is typically performed as an image processing task rather than as a conventional acoustic signal processing problem.

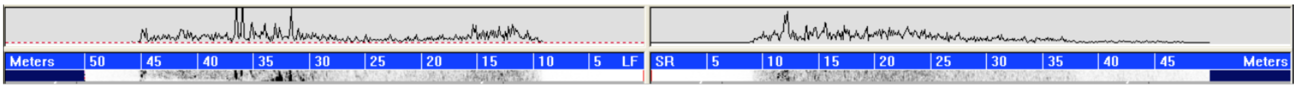

Figure 1. Acoustic seabed backscatter response seen by a sidescan sonar

Sidescan sonar data has several handicaps. Notably, the backscatter time series and imagery of conventional sidescan sonars do not include depth information, except for the depth directly under the transducer. In the absence of other information a horizontal seabed is assumed. Backscatter responses from portions of seabed at different horizontal ranges from the transducer, but with the same slant range, can be received simultaneously, causing imagery to have defects at unknown positions. Features proud of the seabed are seen by an enhanced backscatter response on the side of the feature facing the transducers, and an acoustic shadow on the other side. The shadows enable object detection, and can enhance the contrast of smaller features such as ripples, making them easier to discern, but shadows behind larger features cause a loss of spatial information, and complicate autonomous data processing. A smooth, horizontal seabed is ensonified at a range of incident angles, leading to a non-uniform backscatter response from a homogeneous seabed (tone changes across the swathe – see the left hand image in Figure 2). Movement of the sonar transducer(s) can introduce artefacts to imagery. Spatial resolution changes across the swath, causing distortion in the part of the record closest to the sonar. The sonar beam pattern and side lobes can introduce artefacts, notably near nadir striping.

3. Examples of Sidescan Sonar Imagery

Examples of sidescan sonar imagery are shown in Figures 2 to 6. They show the great variation in scale and texture of sedimentary and geological features.

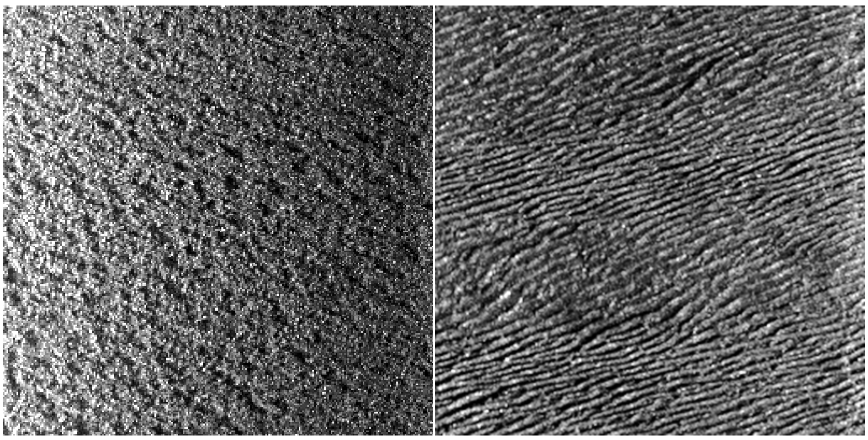

Figure 2. Sandy seabeds characterised by smaller ripples

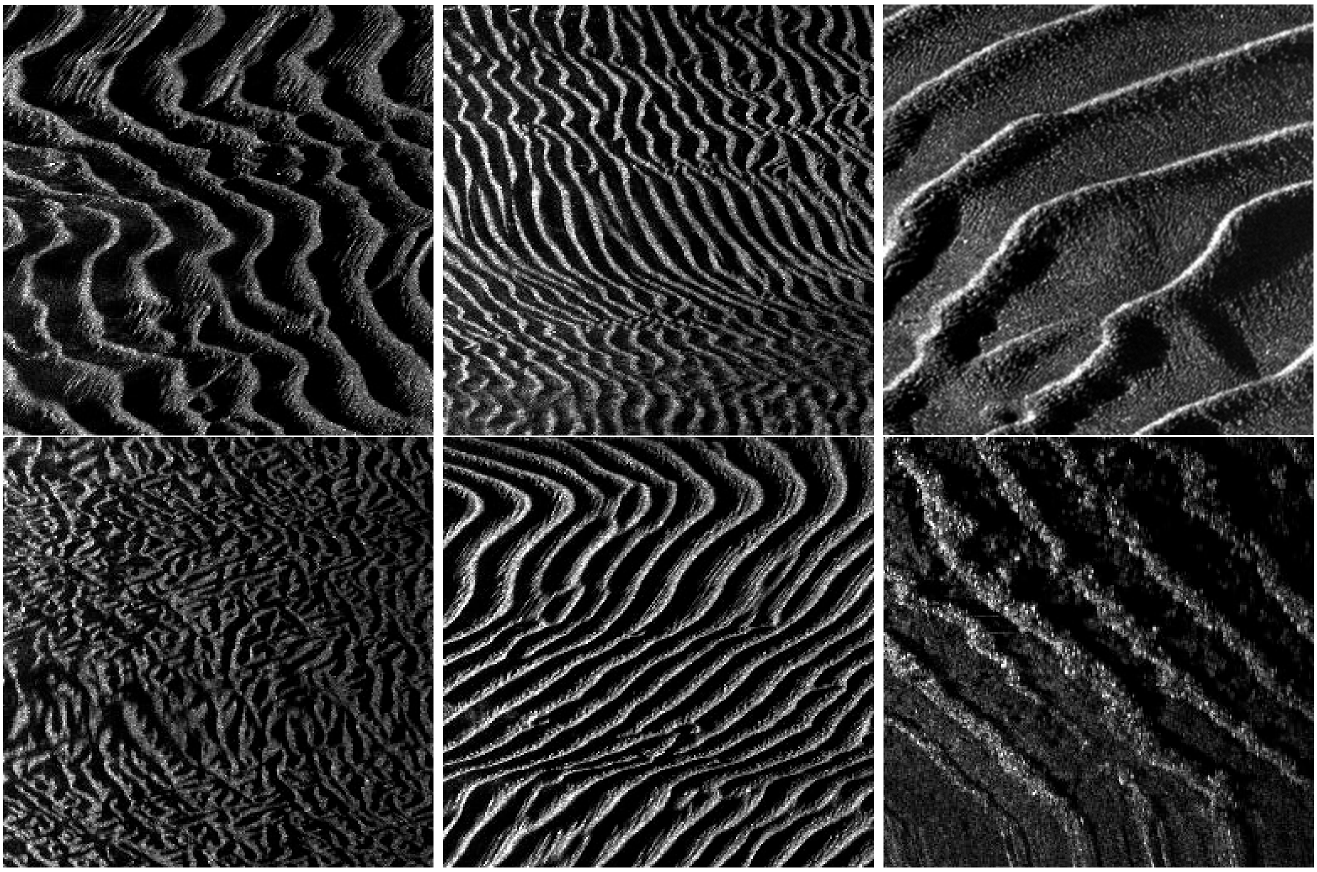

Figure 3. Ripples and sandwaves of various scales and orientations with respect to the sonar

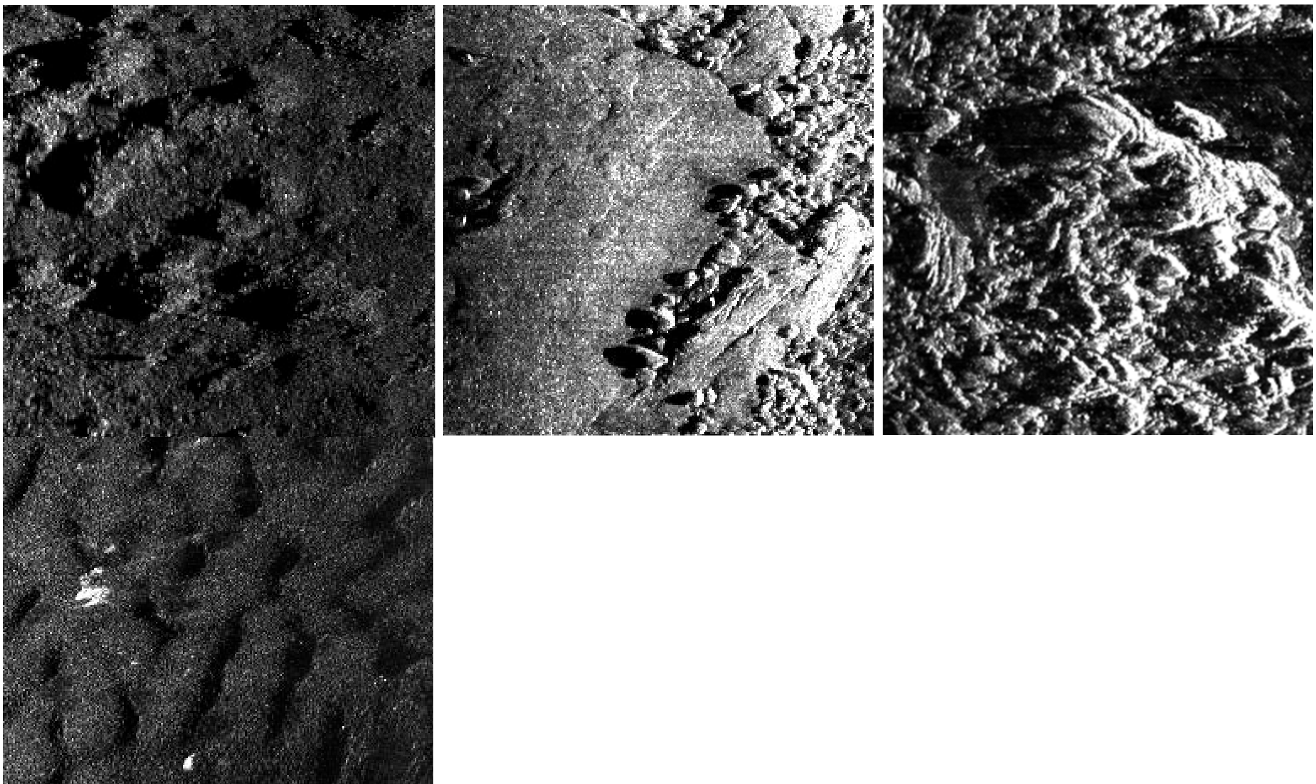

Figure 4. Rough, lumpy, and rocky seabed types

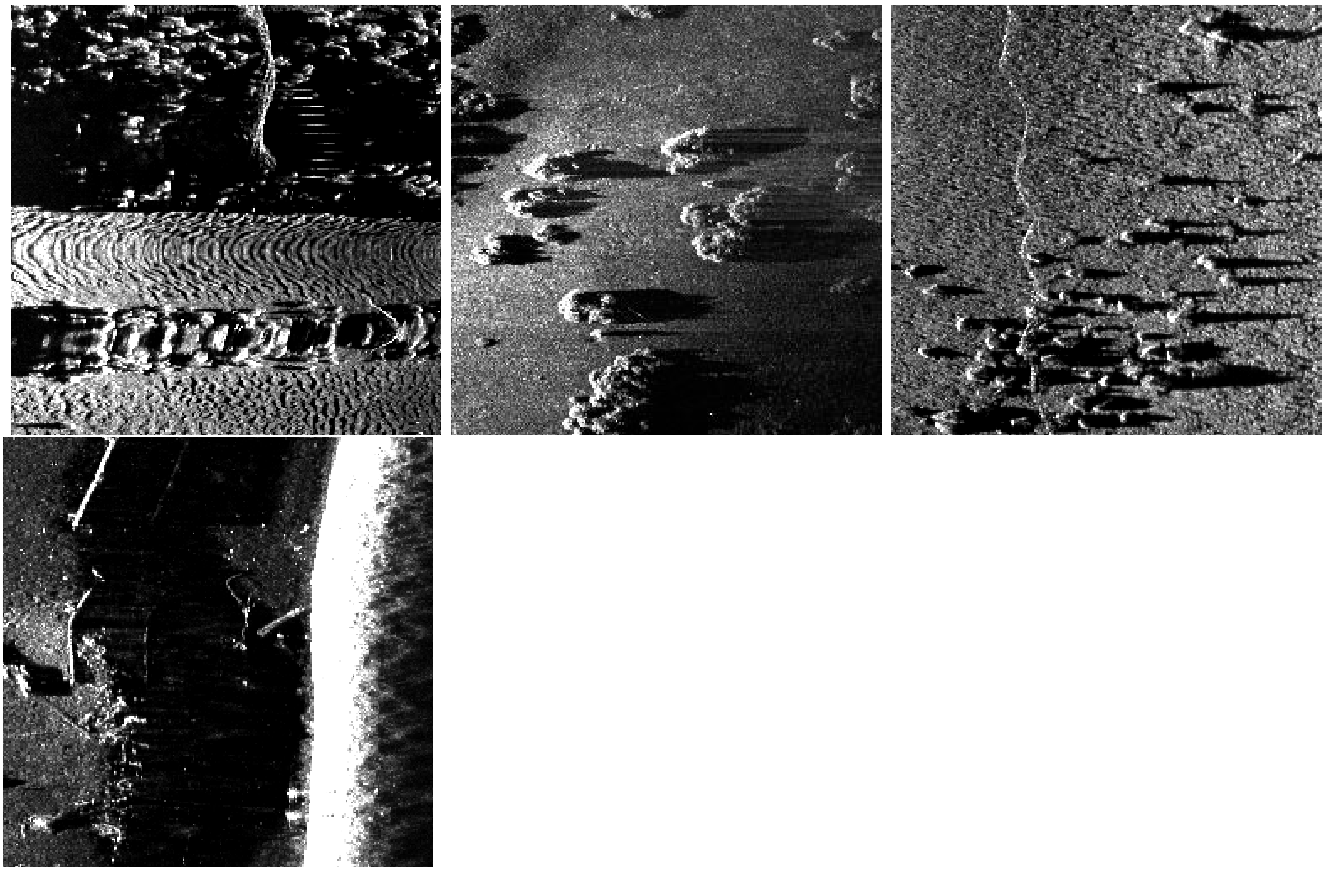

Figure 5. Sidescan sonar imagery with multiple seabed types. From left to right, (top) rock and sand; coral outcrops; a stone field on sand; (bottom) debris and scour adjacent to a wharf

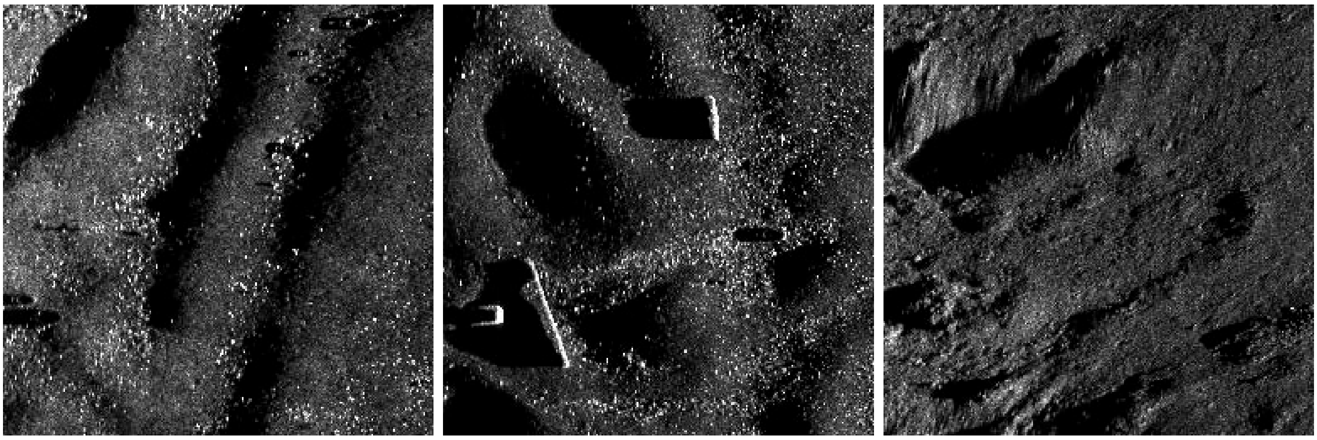

Figure 6. Seabeds with undulatory features and shadow zones (the dark areas)

4. Methods of Processing Sidescan Sonar Imagery

Processing methods are required which can provide information on seabed characteristics with sufficient surety to enable reliable machine decisions on the probability of successful hunting of manmade objects or the presence of particular seabed types. Methods trialled were the GLCM technique (see below), Gaussian Mixture Models, Contour clustering, Backscatter histogrammes. Statistical clustering with the CLARA algorithm of Kaufman and Rousseeuw (1990) was used to handle the data from the large number of test images (77,351 sub-images of 256x256 pixels).

4.1 Gray Level co-occurrence matrix (glcm) method for characterisation of image textures

GLCM is an image processing technique developed by Haralick et al (1973) which analyses texture and tone of pixel based imagery. It has been used for post-processing of sidescan sonar image texture characterization for about 25 years (for example Reed and Hussong (1989), Keeton (1994), Blondel et al (1998)). There are several methods for image texture classification but GLCM is generally reported as superior to them for sidescan sonar data (e.g. Karoui et al 2008). "*GLCMs address the average spatial relationships between pixels of a small region, by quantifying the relative frequency of occurrence of two grey levels at a specified distance and angle from each other. If the image is quantized on NG grey levels, each point of the image will be described with an NG x NG matrix. Because they are difficult to manipulate and interpret, GLCMs are described by statistical measures, called indices. More than 25 are available from the current literature …*)" (Blondel et al 1998). Possible angles are 0, 45, 90, 135°. From Clausi & Zhao (2003), "*Effectively, a two-dimensional histogram is created (dimensioned to G x G* [where G is the number of grey scale levels in the image]*) that represents the total number of occurrences for each (i, j) grey level pair* [i and j are integer grey scale levels] *that occurs in a fixed sized window given a certain spatial (and angular) offset*". "*The co-occurring probabilities are determined by dividing C(i,j)* [the number of occurrences for a particular (i,j) pairing] *by the total number of counts across all i and j*".

Angle 0° was chosen to match the sidescan acquisition geometry, with pixel separation of unity. The 64 grey levels were reduced to 16 (this is termed quantisation). GLCM window and image pixel size must be commensurate with the scale of the seabed texture features or objects being sought. Window sizes were varied from 5x5 pixels to 45x45 pixels. Windows of 17x17 pixels to 23x23 pixels appeared useful for seabed texture, with smaller windows better for delineating smaller details and features. No slant range, beam pattern, or radiometric corrections were made to the imagery.

Examples of GLCM parameters are Angular Second Moment (also known as energy, uniformity, and sometimes as homogeneity and local homogeneity), Contrast (or inertia), Correlation, Variance, Inverse Difference Moment (IDM) (homogeneity, local homogeneity), sum average, sum variance, sum entropy, entropy, difference variance, difference entropy, Dissimilarity (which is similar to contrast), and Maximum Probability (Clausi & Zhao 2003).

Care is needed in GLCM parameter selection. The simplest GLCM usage occurs if a single parameter can be used to characterize imagery. This is not expected to be viable, since some parameters are influenced by both texture and tone, or by more than one specific textural property (Baraldi and Parmiggiani (1995)). For example high Homogeneity (IDM) is calculated for textures with ideal repetitive structures, or if the image has little variation (Gebejes & Huertas (2013)). Alternatively expressed, "*Energy (ASM) reaches its highest value when gray level distribution has either a constant or a periodic form*" (Shokr, 1991). The same values of IDM may therefore describe very different conditions.

Only GLCM parameters which can be given a universal or normalized form are useful to compare images with different grey scale quantisations, shifts, or linear gains. Fully normalized forms are available for Entropy (Bianconi & Fernandez 2014) and ASM. Entropy and ASM are strongly inversely correlated. Contrast and IDM (Shokr 1991), and Correlation (Blondel 1996) can be normalized for gray tone linear transformations. Preferably parameters are also rotation invariant.

The selected GLCM parameters should be largely uncorrelated – tests indicate Correlation is independent of the others, and that others are strongly related. Correlation and Entropy were chosen as normalizable and independent parameters. This enables use of a simple 2-parameter classification space. Correlation tends to find linear features in an image, and Entropy describes order or disorder. A completely random distribution has high entropy, and an image of constant tone has entropy of 0.

GLCMs are computationally intensive, potentially causing problems for real-time operations on autonomous underwater vehicles. C++ coding of Clausi and Zhao (2003) for fast GLCM calculation was used. This code uses hash tables and linked lists to lessen computations for sparse matrices.

4.1.1 Using the GLCM parameters

The two normalized parameters were scaled to 256 integer levels. Counts of combinations of CorrelationValue-EntropyValue were made and displayed as a density plot. The plot was classified by segmenting it into squares, and the resulting classes were plotted in geographical space (Figure 7). Results indicated the GLCM method was useful for segmentation of images, even though classification squares may cut across data trends. The problem is to transform this information into useable form. For example, signatures or templates are required for archetypal seabeds. How many seabed types do we have? Several automatic means were trialled to examine this question.

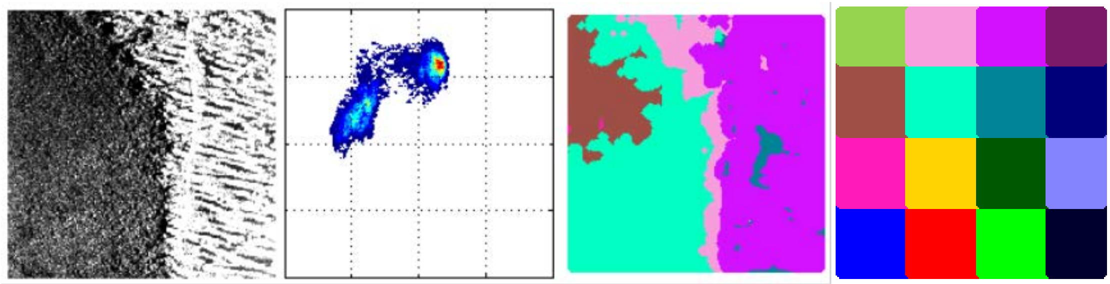

Figure 7. Seabed segmentation with two GLCM parameters (image, 2-parameter classification space, segmented image, colour coding for the classification squares)

4.2 Clustering of counts

The first method clustered the statistical objects formed by vectors of counts of GLCM pair combination falling in classification squares (e.g. a 6x6 segmentation of the classification space has 36 counts) (Figure 8). An unsupervised clustering of the 77,351 vectors of 36 counts was made with the CLARA algorithm (Kaufman and Rousseeuw 1990). This appeared useful, and clustering was then made on finer divisions of the classification space up to 50x50 squares. Up to 99 clusters were formed (it is better to have too many clusters than too few). Some clusters were composed of highly similar images, but others were not, and it was not always clear why.

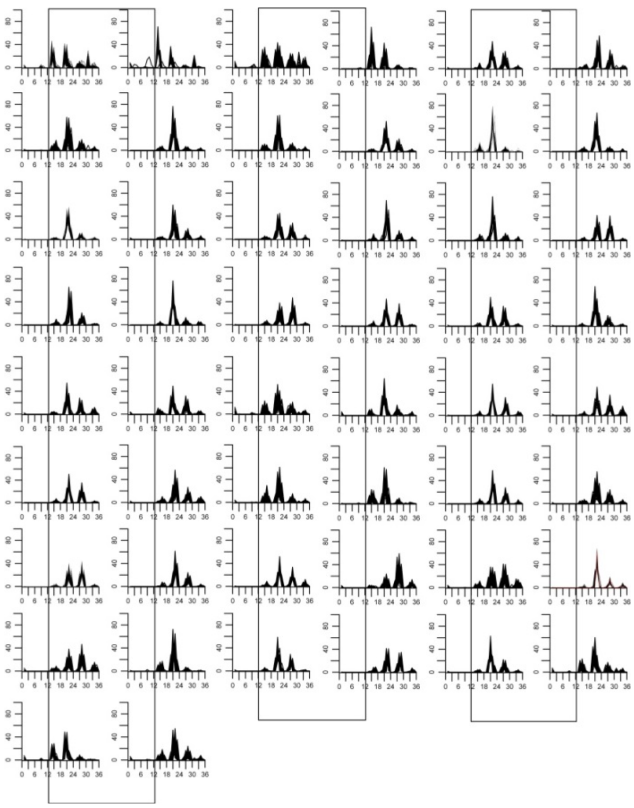

Figure 8. A clustering of vectors of counts of Correlation-Entropy GLCM parameter pairings

4.3 Manual classification using clustering results

Next, clusters of seabed types with uniform backscatter properties and tightly defined GLCM parameter distributions were used to form a manually derived classification scheme, following which counts of parameter-pairs in the manual classification polygons were clustered to form groups of images.

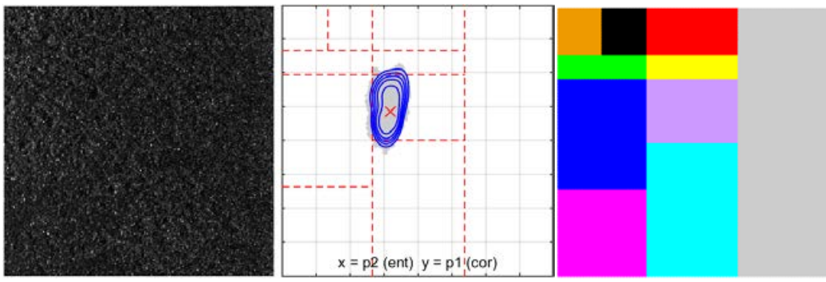

Figure 9. Manual classification (rightmost image) derived from tight GLCM parameter distributions

None of these clusterings was satisfactory for all seabeds. Figure 10 shows a portion of a cluster of images for which all images were similar. Figure 11 shows a portion of a cluster where a good clustering of ripple types was marred by inclusion of a few images completely dissimilar to the ripples. Also, for some sets of similar images with more than one seabed type the overall 2-parameter distributions appeared distinctive, but they were not the sum of the parts. Probable causes are GLCM windows with more than one texture type giving a mixed result, and real gradation in properties between spatially adjacent different types of seabeds.

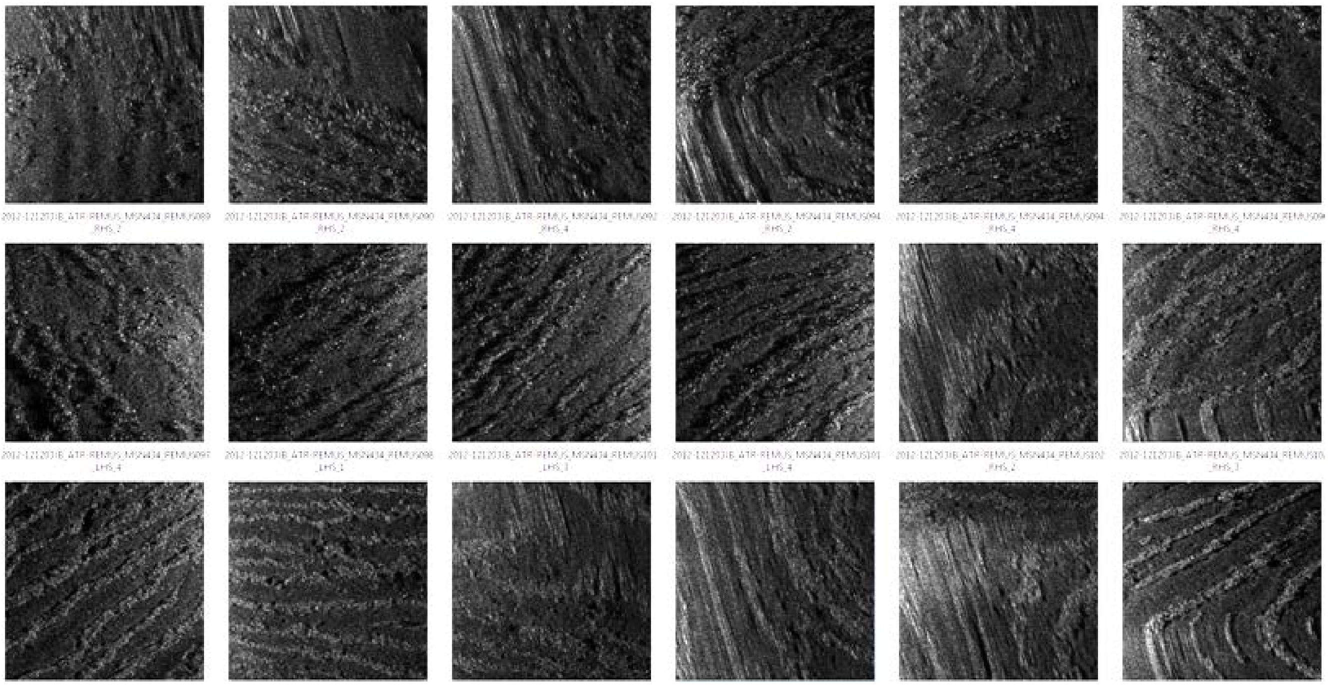

Figure 10. Example of images assigned to the same cluster

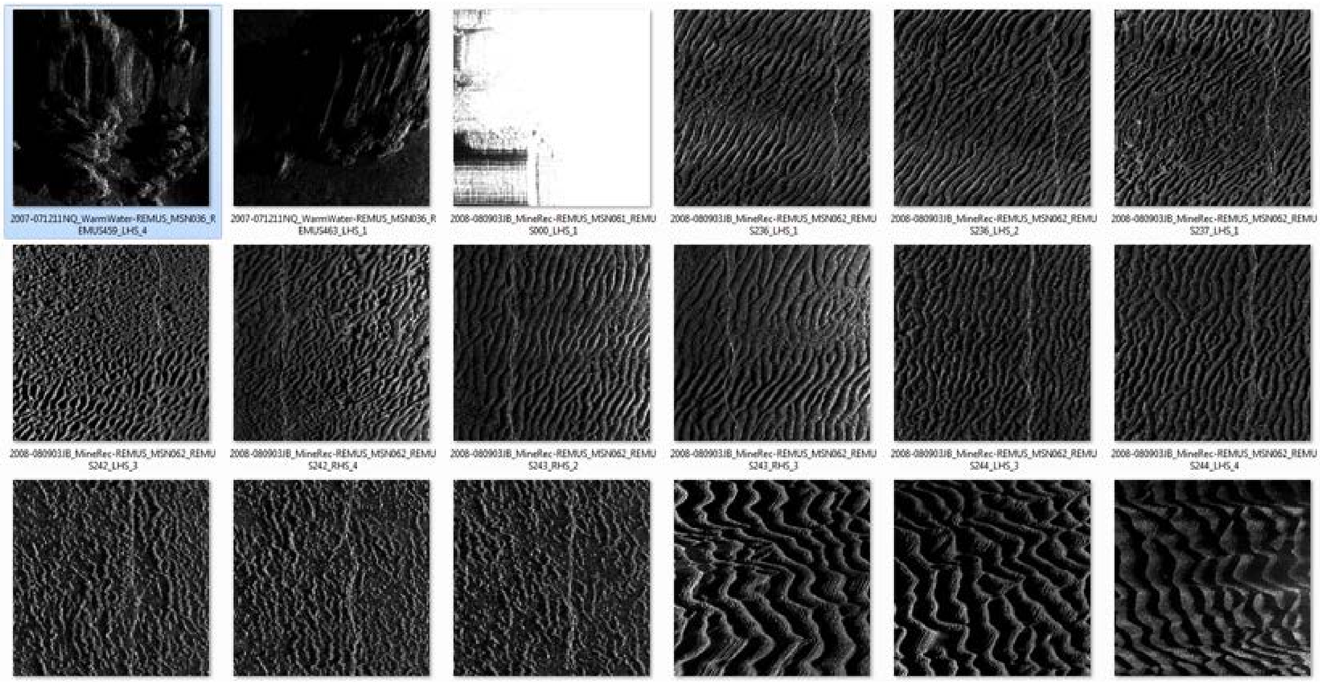

Figure 11. This clustering of ripple images begins with three anomalous images

4.4 Gaussian mixture models (GMMs)

A more sophisticated classification method was then trialled. Gaussian Mixture Models (GMMs) were used to form probability distributions, probability contours, and density centres for the classification space (Figure 12). Because of the diversity of seabed types the GMM locii covered the classification space and were not useful for classification.

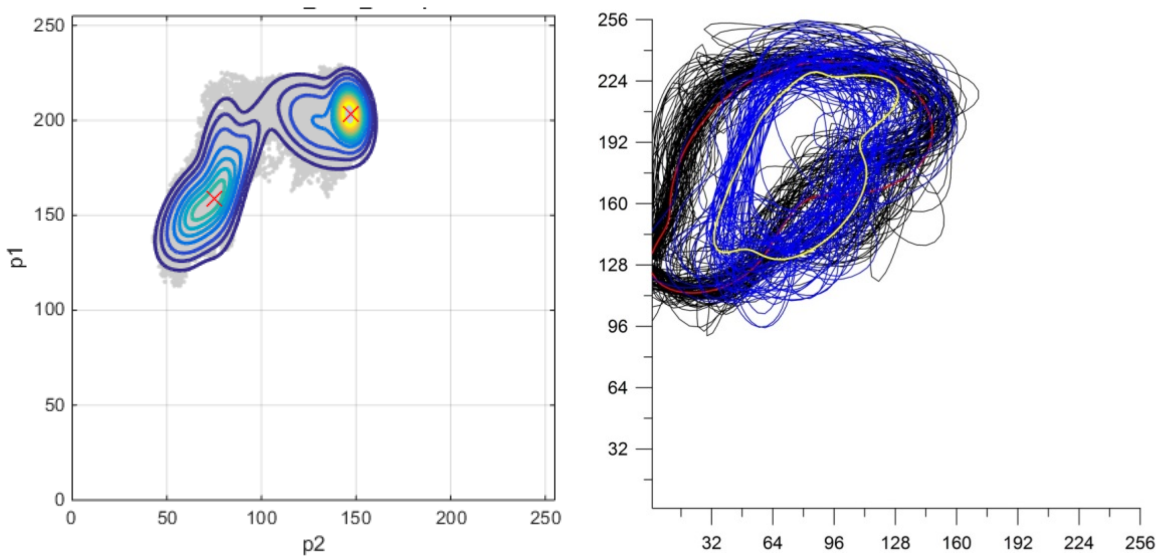

Figure 12. Left: Example of Gaussian Mixture Modelling for the 2-parameter GLCM classification space. Right: Example of clusterings of bounding GMM contours

A statistical clustering was made on the bounding contours of the GMM distributions to see if this was useful to classify mixed seabeds (Figure 12). There are several fast comparison methods to find large and small polygonal figures with similar shapes, regardless of rotation, translation, and scaling with respect to each other. However, the orientations of the GMM contours is fixed, and simple pixel to pixel comparisons were used to decide if bounding contours matched templates (Figure 13). Results were superior to the previous methods, but some clusters still included a variety of seabed types.

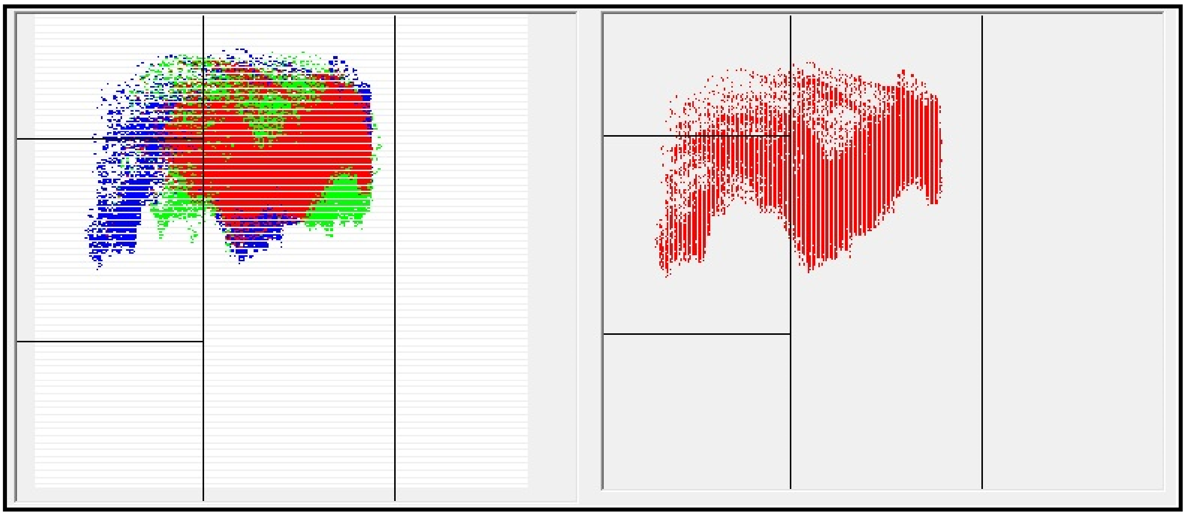

Figure 13. Image masking and pixel counting to compare GLCM parameter distributions with templates. The template is on the right. All non-zero value pixels in the 2-parameter distributions of the image and template classification spaces are set to unity. The masked image is on the left. Red = Left pixel and Right pixel are present in both images, Green = only the Left pixel is present, Blue =only the Right pixel is present. A single user determined threshold is used to decide if a match occurs.

4.5 Clustering of grayscale brightness level histogrammes

A clustering of grayscale brightness histogrammes was then made. GLCM features are said to be superior to grayscale histogramme features, and so it proved for clusterings of sidescan sonar images obtained from the histogrammes. However, it was noted that the histogrammes were useful to filter out some types of bad data such as the third image across from the top left in Figure 11.

5. Discussion and Conclusions

Reliable classification templates have so far been found only for some seabeds which have more even textures, and for some particular combinations of seabed types. Present indications are that a classification based on two GLCM parameters may not be quite sufficient to enable autonomous characterization of seabed type. This is principally because of the great diversity of scales and textures of seabed types, but also because of the limitations of any texture based method utilising pixel relationships.

What next? Characterization of sidescan sonar imagery to enable autonomous decisions by UUVs is likely to be an evolutionary process. The simple approach to finding templates for autonomous seabed classification through statistical clustering of probability contours in the classification space appears the most likely of the 2-parameter methods to succeed, but it may need augmentation through addition of a third parameter, and a more probabilistic approach. The deficiencies of sidescan sonar mean that not every seabed type can be definitively or reliably classified. Bathymetric estimations from Shape From Shading and from geometrical techniques using the dimensions of acoustic shadows may provide useful additions to the texture information available in sidescan sonar imagery.

References

[1] Baraldi, A. and Parmiggiani, F. “An investigation of the textural characteristics associated with gray level co-occurrence matrix statistical parameters”, *IEEE Transactions on Geoscience and Remote Sensing*, **33**(2), 293-304, (1995).

[2] Bianconi, F. and Fernández, A. “Rotation invariant co-occurrence features based on digital circles and discrete Fourier transform”, *Pattern Recognition Letters*, **48**, 34-41, (2014).

[3] Blondel, P. "*Segmentation of the Mid-Atlantic Ridge south of the Azores, based on acoustic classification of TOBI data*", Pages 17-28 in C.J. MacLeod, P.A. Tyler, C.L. Walker. (eds). Tectonic, Magmatic, Hydrothermal and Biological Segmentation of Mid-ocean Ridges. Geological Society Special Publication No. 118, (1996).

[4] Blondel, P. "Automatic mine detection by textural analysis of COTS sidescan sonar imagery". *International Journal of Remote Sensing,* **21**(16), 3115-3128, (2000).

[5] Clausi, D.A. and Zhao, Y. "Grey level co-occurrence integrated algorithm (GLCIA): a superior computational method to rapidly determine co-occurrence probability texture features", *Computers & Geosciences,* **29**, 837-850, (2003).

[6] Gebejes, A. and Huertas, R. "Texture characterization based on grey-level co-occurrence matrix", *Proceedings of the Conference of Informatics and Management Sciences*, ICTIC 2013, Slovakia, 25-29 March 2013, pp. 375-37.

[7] Hamilton, L.J. and Parnum, I. "Seabed segmentation from unsupervised statistical clustering of entire multibeam sonar backscatter curves", *Continental Shelf Research,* **31**(2), 138-148, (2011).

[8] Haralick, R.M., Shanmugam, K. and Dinstein, R. "Textural features for image classification", *IEEE Transactions on Systems, Man, And Cybernetics,* **3**(6), 610-621, (1973).

[9] Karoui, I., Fablet, R., Boucher, J.-M. and Augustin, J.-M. "Seabed segmentation using optimised statistics of sonar textures", *IEEE Transactions on Geoscience and Remote Sensing*, **47**(6), 1621-1631, (2009).

[10] Keeton, J.A. T*he use of image analysis techniques to characterise mid-ocean ridges from multibeam and sidescan sonar data*, PhD Thesis, University of Durham, 1994.

[11] Reed, T.B. and Hussong, D. "Digital image processing techniques for enhancement and classification of SeaMARC II sidescan sonar imagery", *Journal of Geophysical Research,* **94**, 7469-7490, (1989).

[12] Shokr, M.E. "Evaluation of second-order texture parameters for sea ice classification from radar images", *Journal of Geophysical Research,* **96**, 10625-10640, (1991).